

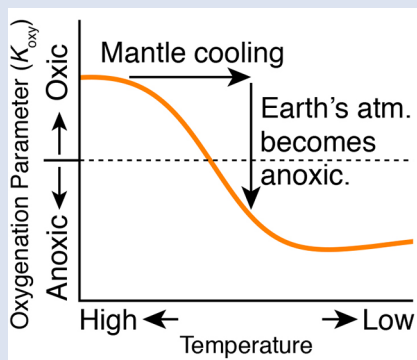
Mantle cooling causes more reducing volcanic gases and gradual reduction of the atmosphere

S. Kadoya^{1*}, D.C. Catling¹, R.W. Nicklas³, I.S. Puchtel², A.D. Anbar⁴



doi: 10.7185/geochemlet.2009

Abstract



The early atmosphere contained negligible O₂ until the Great Oxidation Event (GOE) around 2.4 Ga, but evidence suggests that production of photosynthetic O₂ began hundreds of millions of years earlier. Thus, an ongoing debate concerns the trigger of the GOE. One possibility is that volcanic gases became more oxidising over time. Secular cooling of the mantle affects thermodynamic equilibria and also changes the proportions of reduced and oxidised volcanic gases. Here, we examine the consequences of mantle cooling for the evolution of Earth's atmospheric redox state. Contrary to some previous hypotheses, we show that as the mantle cools, volcanic emissions contain a greater proportion of reducing gases, which produces a more reducing atmosphere. However, the atmosphere became more oxic. Therefore, the redox consequences of other processes, such as secular oxidation of the mantle and/or hydrogen escape to space, must have dominated over that of mantle cooling in shaping the redox evolution of Earth's atmosphere.

Received 11 October 2019 | Accepted 12 February 2020 | Published 16 March 2020

Introduction

The partial pressure of Archean atmospheric O₂ was $<0.2 \times 10^{-6}$ bar and rose during the Great Oxidation Event (GOE), between 2.4 Ga and 2.1 Ga, as indicated by the disappearance of mass independent sulfur isotope fractionation in sedimentary rocks (Farquhar *et al.*, 2000; Pavlov and Kasting, 2002; Zahnle *et al.*, 2006). However, chromium, iron, and molybdenum isotope data suggest the presence of O₂ in the marine photic zone (oxygen oases) as early as ~3 Ga (Planavsky *et al.*, 2014; Satkoski *et al.*, 2015), and evidence exists for mild oxygenation from these and other proxies at 2.5 Ga (Ostrander *et al.*, 2019 and references therein). Evidence for free O₂ before the GOE is also consistent with phylogenetic inferences that oxygenic photosynthesis evolved by the mid to late Archean (Schirmeister *et al.*, 2015; Magnabosco *et al.*, 2018); earlier, anoxygenic photosynthesis would have been present (Sleep, 2018).

The reason for the apparent time lag between the advent of oxygenic photosynthesis and the GOE is debated (Catling *et al.*, 2001; Holland, 2002; Kump and Barley, 2007; Holland, 2009; Gaillard *et al.*, 2011; Kasting, 2013; Ciborowski and Kerr, 2016; Lee *et al.*, 2016; Brounce *et al.*, 2017; Duncan and Dasgupta, 2017; Moussallam *et al.*, 2019). One possibility is that if ancient volcanic gases were sufficiently reducing, they

would have overwhelmed O₂ production fluxes, limiting O₂ to trace levels. If volcanic gases became gradually more oxidised, atmospheric O₂ would accumulate rapidly at a tipping point when the reducing volcanic gas flux fell below the O₂ production flux (Holland, 2002; Claire *et al.*, 2006).

Several hypotheses account for gradual oxidation of volcanic gases: the oxidation of the mantle as a consequence of hydrogen escape to space (Kasting *et al.*, 1993); a decrease in volcanic degassing pressure associated with an increase in subaerial volcanoes (Kump and Barley, 2007; Gaillard *et al.*, 2011) though this hypothesis is contradicted by Brounce *et al.* (2017); increasing CO₂ and/or SO₂ degassing due to increased subduction of carbonate and sulfate sediments (Holland, 2002, 2009) or plume magmatism (Ciborowski and Kerr, 2016); and/or an increase in recycling of organic material (Duncan and Dasgupta, 2017).

Recently, Moussallam *et al.* (2019) suggested that a decrease in volcanic emission temperature, which they defined as that of the fumarole where gases enter the air, caused volcanic gases to become more oxidised. They argued that the secular cooling of the planetary interior caused a decrease in emission temperatures, oxidation of volcanic gases, and the GOE. Specifically, they considered the cooling of a parcel of gas in a volcanic vent as a closed system separated from a melt.

1. Department of Earth and Space Sciences / cross-campus Astrobiology Program, University of Washington, Box 351310, Seattle, WA 98195-1310, USA
 2. Department of Geology, University of Maryland, College Park, MD 20742, USA
 3. Geoscience Research Division, Scripps Institution of Oceanography, La Jolla, CA 92093, USA
 4. School of Earth and Space Exploration and School of Molecular Sciences, Arizona State University, Tempe, AZ 85287, USA
- * Corresponding author (email: shintaro.kadoya@gmail.com)



Here, we examine how cooling affected volcanic gas buffered by a surrounding melt and gases in a subsequent closed system. We analyse the effect of inferred changes in the proportions of oxidised and reduced volcanic gases on the redox state of the atmosphere.

Model

We begin by describing our model briefly. Supplementary Information Section S-1 contains additional details. We assume that volcanic gas consists of H₂O, H₂, CO₂, CO, CH₄, SO₂, and H₂S in thermodynamic equilibrium at a total pressure of 5 bar, assuming a subaerial volcanic eruption (Holland, 1984; p. 47). Section S-8 discusses how the redox state of volcanic gases changes outside of this nominal pressure value. Partial pressures of the gas species are calculated using mass conservation of hydrogen, carbon, and sulfur, and relevant thermodynamic equilibria (see also Section S-1.1).

We model two end members of the redox state of the gas mixture. This redox state corresponds to the amount of oxygen within the gas mixture, which is described in our two cases as follows. In one case, the “buffered system”, the gas interacts with surrounding melt and rocks. Oxygen exchanges with the melt such that O₂ fugacity is fixed at a given temperature and pressure. For the other case, the “closed system”, we assume that the gas and its reactions are isolated from the melt, and since no constituents are supplied or released, we conserve mass for oxygen, hydrogen, carbon, and sulfur (Supplementary Information Eq. S-12; see also Eq. S-6, S-7 and S-8).

We evaluate the oxygenation effect of volcanic gas using an oxygenation parameter, K_{oxy} , introduced in previous studies (Catling and Claire, 2005; Claire *et al.*, 2006; Kasting, 2013). This parameter is the ratio of the source flux of O₂ (F_{source}) to the kinetically rapid sink flux of O₂ (F_{sink}):

$$K_{\text{oxy}} \equiv \frac{F_{\text{source}}}{F_{\text{sink}}} \quad \text{Eq. 1}$$

Here, F_{sink} corresponds to degassing of reductive, *i.e.* oxidisable, volcanic gases, which can include an excess of reductants beyond that which reacts with O₂.

By construction, F_{source} and F_{sink} are not meant to balance each other: they omit fluxes that depend on atmospheric redox state, such as hydrogen escape to space in F_{source} and oxidative weathering, *e.g.*, oxidation of Fe²⁺ to Fe³⁺, in F_{sink} (Catling and Claire, 2005; Kasting, 2013). When $K_{\text{oxy}} < 1$, O₂ sinks exceed O₂ sources and excess H₂ accumulates until balanced by escape to space. When $K_{\text{oxy}} > 1$, O₂ sources exceed O₂ sinks and O₂ accumulates until balanced by oxidative weathering. The evolution of K_{oxy} in a box model coupled to photochemistry shows how atmospheric oxygenation occurs when K_{oxy} reaches unity (Claire *et al.*, 2006).

We assume that oxygenic photosynthesis is present because we are evaluating O₂ build up. We consider H₂O, CO₂, and SO₂ to be redox neutral, while H₂, CO, CH₄, and H₂S fluxes consume O₂ in atmospheric photochemistry. The burial of organic matter and pyrite (FeS₂) are O₂ source fluxes. Considering the stoichiometry of O₂ consumption and production, we rewrite Eq. 1 as follows (derived in Section S-1):

$$K_{\text{oxy}} \equiv \frac{4f_{\text{org}} \times (p\text{CO}_2 + p\text{CO} + p\text{CH}_4) + 5p\text{SO}_2}{2p\text{H}_2 + 2p\text{CO} + 8p\text{CH}_4 + p\text{H}_2\text{S}} \quad \text{Eq. 2}$$

Here, f_{org} represents the fraction of carbon buried as sedimentary organic carbon. Although f_{org} has changed with time, for a nominal case, we set f_{org} to 20 %, which is a rough average over geologic time (Krissansen-Totton *et al.*, 2015). Section S-7 discusses the dependence of K_{oxy} on variations of f_{org} . The

mechanism that sets f_{org} is beyond our scope. However, f_{org} might be controlled by divalent cation fluxes that modulate the carbonate burial flux, which complements the organic burial flux (Sleep, 2005).

Results and Discussion

The degassing process has two stages. Firstly, a gas bubble emerges from melt. The oxygen fugacity of this gas mixture is buffered by the surrounding melt since gases react with the melt. So, this stage corresponds to the buffered system case. Secondly, the bubble ascends within the melt, and the gas temperature adiabatically decreases with decompression (Oppenheimer *et al.*, 2018). In this stage, gases react with each other within the closed system bubble. Hereafter, we explain the redox speciation of volcanic gases during each stage.

First, we consider the oxidation state of global volcanic gas emissions for the buffered system. We define the redox state as the difference of logarithm of f_{O_2} from that of the Quartz-Fayalite-Magnetite (QFM) buffer: $\Delta\text{QFM} = \log_{10} f_{\text{O}_2} - \log_{10} f_{\text{O}_2, \text{qfm}}$. Also, we consider 4 different redox states of the surrounding melt (and rocks), and we assume that the redox state of the surroundings in each case is constant and independent of temperature. Since we consider cooling from 2000 K, we denote the oxidation state of the melt as ΔQFM_{2000} . The choice of the initial temperature is arbitrary and does not affect our conclusions.

The ΔQFM of the gas is equal to the ΔQFM of the surroundings and is temperature independent (Fig. 1a) because of buffering by the surrounding melt and rocks. However, since the reference f_{O_2} of the QFM buffer decreases with cooling (Fig. S-1a), the absolute f_{O_2} value of gas and melt decreases with cooling even though their ΔQFM values are constant.

The corresponding K_{oxy} value tells us whether atmospheric oxygenation occurs. K_{oxy} depends on gas composition (Eq. 2), which depends on the equilibrium constant of each reaction in addition to f_{O_2} . Equilibrium constants also depend on temperature (Fig. S-1b). Consequently, cooling causes oxidation of CO to CO₂ and reduction of SO₂ to H₂S (Fig. S-1c), even though the redox buffer relative to QFM is constant (see also Section S-2). The net effect of these opposing changes is a step-like decrease in K_{oxy} with cooling, as shown in Figure 1b. In particular, for the case with $\Delta\text{QFM} = -0.5$, cooling decreases K_{oxy} from >1 to <1 (dashed line, Fig. 1b), which would cause the atmosphere to flip from oxic to reducing.

Now consider a parcel of volcanic gases separated from a melt, *e.g.*, in a volcanic vent. For this closed system gas composition, we calculate an equivalent ΔQFM using the mole ratio of gas species, such as H₂ / H₂O (Section S-4). Cooling changes the ΔQFM (Fig. 2a), unlike in the buffered system (Fig. 1a). In particular, for relatively oxidised cases (*i.e.* $\Delta\text{QFM}_{2000} = 0$ and -0.5), ΔQFM increases with cooling (solid and dashed lines in Fig. 2a), consistent with the results of Moussallam *et al.* (2019). However, for relatively reduced cases (*i.e.* $\Delta\text{QFM}_{2000} = -1$ and -1.5), the change in ΔQFM is moderate (dash-dot and dashed lines in Fig. 2a). The increase in ΔQFM with cooling in the closed system occurs because reduction of SO₂ to H₂S is accompanied by oxidation of H₂ to H₂O by redox conservation (Section S-3). Consequently, the ratio $p\text{H}_2 / p\text{H}_2\text{O}$ declines, producing a relative increase in f_{O_2} (see Sections S-3 and S-4).

K_{oxy} also changes with cooling of the closed system gas (Fig. 2b). However, within the closed system, reduction of one gas is accompanied by oxidation of another gas. Consequently, temperature dependent reactions within a closed system gas mixture do not change the overall sink of O₂ in the gas mixture, contrary to the conclusions of Moussallam *et al.* (2019).



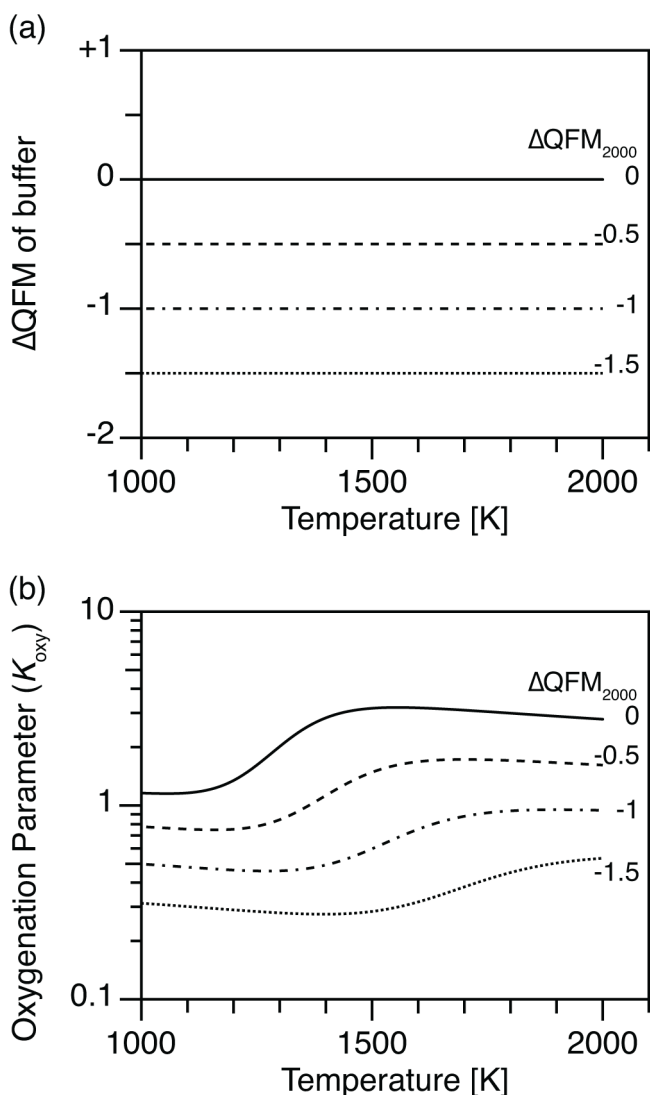


Figure 1 (a) Oxidation state (ΔQFM) buffering volcanic gas composition, and (b) oxygenation parameter (K_{oxy}), as a function of temperature. Here, we assume a system where gases are redox buffered by the surrounding melt and rocks. ΔQFM_{2000} represents the oxidation state at 2000 K. By definition, ΔQFM is independent of temperature and equal to ΔQFM_{2000} in (a) whereas cooling tends to decrease K_{oxy} in (b).

For example, consider a mixture initially containing 1 mol of SO_2 and 3 mol of H_2 , where all SO_2 is reduced, $SO_2 + 3H_2 \rightarrow H_2S + 2H_2O$ (see also Section S-3). The moles of O_2 that can be consumed by the gas mixture do not change. Reduction of 1 mol SO_2 accompanied by oxidation of 3 mol H_2 decreases the overall sink of O_2 by 0.25 mol O_2 but the production of 1 mol H_2S compensates.

A subtlety is that although the O_2 sink cannot change, K_{oxy} shifts because K_{oxy} also accounts for global O_2 sources from converted volcanic gases. In our ‘toy’ example, 1 mol SO_2 corresponds to a 1.25 mol O_2 source (see Section S-1.2), while 3 mol of H_2 and 1 mol of H_2S correspond to 1.5 mol O_2 and 0.25 mol O_2 sinks, respectively. Hence, the initial K_{oxy} is $1.25 / 1.5 = 5 / 6$, but after reactions, K_{oxy} becomes $0 / 0.25 = 0$. Here, the expected reduction of SO_2 to pyrite in the global environment (Eq. S-18) is the source of O_2 that changes K_{oxy} . The important point is that an initial K_{oxy} of <1 remains less than unity.

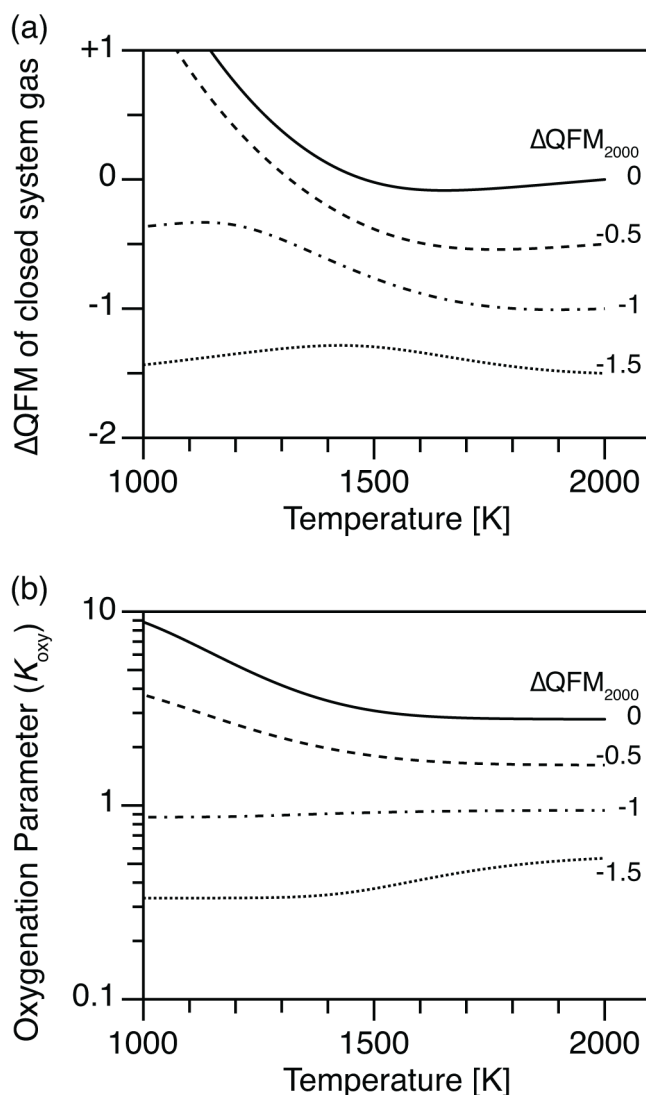


Figure 2 (a) Oxidation state (ΔQFM), and (b) oxygenation parameter (K_{oxy}), as a function of temperature. Here, we assume a closed system of gases, and the ΔQFM of the gases at 2000 K is denoted as ΔQFM_{2000} . Cooling changes ΔQFM unlike the melt buffered case (Fig. 1a) and changes K_{oxy} . However, an initial K_{oxy} that exceeds unity remains >1 with cooling, and an initial K_{oxy} that is less than unity remains <1 .

Consider again Figure 2. Temperature dependent gas reactions within a closed system do not change the overall sink of O_2 in the gas mixture. For relatively oxidised cases ($\Delta QFM_{2000} = 0$ and -0.5), cooling increases K_{oxy} (solid and dashed lines in Fig. 2b). However, for relatively reduced cases ($\Delta QFM_{2000} = -1$ and -1.5), cooling decreases K_{oxy} (dash-dot and dotted lines in Fig. 2b). In summary, an initial K_{oxy} of >1 remains larger than unity with cooling, while an initial K_{oxy} of <1 stays less than unity (Fig. 2b).

Therefore, reactions under a melt buffer system change the capacity of the gas to consume O_2 and affect atmospheric oxygenation while reactions within the closed system cannot. So, the oxygenation effect of volcanic degassing depends on interactions with the melt.

The Earth’s interior likely cooled with time (Bickle, 1982; Nisbet *et al.*, 1993; Herzberg *et al.*, 2010; Aulbach and Arndt, 2019). However, even if the upper mantle’s oxidation state was constant (e.g., $\Delta QFM = -0.5$), its cooling would decrease K_{oxy}

and even reduce the atmosphere (Fig. 1b). Thus, processes that dominate over such a K_{oxy} decrease are required to explain the GOE.

The trigger for the GOE is debated (Kasting *et al.*, 1993; Catling *et al.*, 2001; Holland, 2002; Gaillard *et al.*, 2011; Moussallam *et al.*, 2019). Proposed secular oxidation of the upper mantle caused by hydrogen escape (Kasting *et al.*, 1993) has been dismissed for about two decades because evidence appeared to show a constant oxidation state of the upper mantle (Canil, 1997; Delano, 2001; Canil, 2002; Lee *et al.*, 2005). However, two recent studies suggest that the upper mantle ΔQFM increased by $\sim 1.5 \log_{10}$ units since the early Archean (Aulbach and Stagno, 2016; Nicklas *et al.*, 2019). Such oxidation would cause K_{oxy} to increase and so possibly triggered the GOE. Regardless, we have shown that if mantle ΔQFM does not increase, mantle cooling actually makes the atmosphere more reducing, contrary to previous claims that mantle cooling would trigger the GOE (Moussallam *et al.*, 2019).

Conclusions

We examined the effects of Earth's secular cooling and volcanic gases on oxygenation of the atmosphere using an oxygenation parameter, K_{oxy} , that is less than unity for an anoxic atmosphere and exceeds unity for an oxic atmosphere (Catling and Claire, 2005; Kasting, 2013). Low temperature favours H_2S more than SO_2 because both equilibria constants and the absolute O_2 fugacity of the QFM buffer depend on temperature. Hence, for a buffered system, cooling increases the $p\text{H}_2\text{S} / p\text{SO}_2$ ratio in volcanic gases and decreases K_{oxy} . For a closed system of gases in a vent that is not melt buffered, cooling also increases the $p\text{H}_2\text{S} / p\text{SO}_2$ ratio but this is counteracted by a decrease in $p\text{H}_2 / p\text{H}_2\text{O}$. Hence, cooling of a closed system parcel of gas does not change the overall capacity of the volcanic gases to consume O_2 .

We conclude that the long term cooling of the mantle induced changes in volcanic gas composition that reduced the atmosphere. However, other processes dominated because the atmosphere oxygenated with time. Possibilities include secular oxidation of the mantle (Aulbach and Stagno, 2016; Nicklas *et al.*, 2019) and/or growth in the O_2 source flux due to higher rates of organic carbon burial (relative to oxidant burial) (Kris-sansen-Totton *et al.*, 2015).

Acknowledgements

Funding support came from NSF Frontiers in Earth System Dynamics award No. 1338810.

Editor: Ambre Luguet

Additional Information

Supplementary Information accompanies this letter at <http://www.geochemicalperspectivesletters.org/article2009>.



This work is distributed under the Creative Commons Attribution Non-Commercial No-Derivatives 4.0 License, which permits unre-

stricted distribution provided the original author and source are credited. The material may not be adapted (remixed, transformed or built upon) or used for commercial purposes without written permission from the author. Additional information is available at <http://www.geochemicalperspectivesletters.org/copyright-and-permissions>.

Cite this letter as: Kadoya, S., Catling, D.C., Nicklas, R.W., Puchtel, I.S., Anbar, A.D. (2020) Mantle cooling causes more reducing volcanic gases and gradual reduction of the atmosphere. *Geochem. Persp. Lett.* 13, 25–29.

References

- AULBACH, S., ARNDT, N.T. (2019) Eclogites as palaeodynamic archives: Evidence for warm (not hot) and depleted (but heterogeneous) Archean ambient mantle. *Earth and Planetary Science Letters* 505, 162–172.
- AULBACH, S., STAGNO, V. (2016) Evidence for a reducing Archean ambient mantle and its effects on the carbon cycle. *Geology* 44, 751–754.
- BICKLE, M.J. (1982) The magnesian contents of komatiitic liquids. In: Arndt, N.T., Nisbet, E.G. (Eds.), *Komatiites*. Allen and Unwin, London, 477–494.
- BROUNCE, M., STOLPER, E., EILER, J. (2017) Redox variations in Mauna Kea lavas, the oxygen fugacity of the Hawaiian plume, and the role of volcanic gases in Earth's oxygenation. *Proceedings of the National Academy of Sciences of the United States of America* 114, 8997–9002.
- CANIL, D. (1997) Vanadium partitioning and the oxidation state of Archean komatiite magmas. *Nature* 389, 842–845.
- CANIL, D. (2002) Vanadium in peridotites, mantle redox and tectonic environments: Archean to present. *Earth and Planetary Science Letters* 195, 75–90.
- CATLING, D.C., CLAIRE, M.W. (2005) How Earth's atmosphere evolved to an oxic state: A status report. *Earth and Planetary Science Letters* 237, 1–20.
- CATLING, D.C., ZAHNLE, K.J., MCKAY, C.P. (2001) Biogenic methane, hydrogen escape, and the irreversible oxidation of early Earth. *Science* 293, 839–843.
- CIBOROWSKI, T.J.R., KERR, A.C. (2016) Did mantle plume magmatism help trigger the Great Oxidation Event? *Lithos* 246, 128–133.
- CLAIRE, M.W., CATLING, D.C., ZAHNLE, K.J. (2006) Biogeochemical modelling of the rise in atmospheric oxygen. *Geobiology* 4, 239–269.
- DELANO, J.W. (2001) Redox history of the Earth's interior since similar to 3900 Ma: Implications for prebiotic molecules. *Origins of Life and Evolution of the Biosphere* 31, 311–341.
- DUNCAN, M.S., DASGUPTA, R. (2017) Rise of Earth's atmospheric oxygen controlled by efficient subduction of organic carbon. *Nature Geoscience* 10, 387–+.
- FARQUHAR, J., BAO, H.M., THIEMENS, M. (2000) Atmospheric influence of Earth's earliest sulfur cycle. *Science* 289, 756–758.
- GAILLARD, F., SCAILLET, B., ARNDT, N.T. (2011) Atmospheric oxygenation caused by a change in volcanic degassing pressure. *Nature* 478, 229–U112.
- HERZBERG, C., CONDIE, K., KORENAGA, J. (2010) Thermal history of the Earth and its petrological expression. *Earth and Planetary Science Letters* 292, 79–88.
- HOLLAND, H.D. (1984) *The chemical evolution of the atmosphere and oceans*. Princeton University Press, Princeton, NJ.
- HOLLAND, H.D. (2002) Volcanic gases, black smokers, and the Great Oxidation Event. *Geochimica et Cosmochimica Acta* 66, 3811–3826.
- HOLLAND, H.D. (2009) Why the atmosphere became oxygenated: A proposal. *Geochimica et Cosmochimica Acta* 73, 5241–5255.
- KASTING, J.F. (2013) What caused the rise of atmospheric O_2 ? *Chemical Geology* 362, 13–25.
- KASTING, J.F., EGGLE, D.H., RAEBURN, S.P. (1993) Mantle Redox Evolution and the Oxidation-State of the Archean Atmosphere. *Journal of Geology* 101, 245–257.
- KRISSANSEN-TOTTON, J., BUICK, R., CATLING, D.C. (2015) A Statistical Analysis of the Carbon Isotope Record from the Archean to Phanerozoic and Implications for the Rise of Oxygen. *American Journal of Science* 315, 275–316.
- KUMP, L.R., BARLEY, M.E. (2007) Increased subaerial volcanism and the rise of atmospheric oxygen 2.5 billion years ago. *Nature* 448, 1033–1036.
- LEE, C.T.A., LEEMAN, W.P., CANIL, D., LI, Z.X.A. (2005) Similar V/Sc systematics in MORBs and arc basalts: Implications for oxygen fugacities of their mantle source regions. *Geochimica et Cosmochimica Acta* 69, A639–A639.
- LEE, C.T.A., YEUNG, L.Y., MCKENZIE, N.R., YOKOYAMA, Y., OZAKI, K., LENARDIC, A. (2016) Two-step rise of atmospheric oxygen linked to the growth of continents. *Nature Geoscience* 9, 417–+.
- MAGNABOSCO, C., MOORE, K.R., WOLFE, J.M., FOURNIER, G.P. (2018) Dating phototrophic microbial lineages with reticulate gene histories. *Geobiology* 16, 179–189.



- MOUSSALLAM, Y., OPPENHEIMER, G., SCAILLET, B. (2019) On the relationship between oxidation state and temperature of volcanic gas emissions. *Earth and Planetary Science Letters* 520, 260-267.
- NICKLAS, R.W., PUCHTE, I.S., ASH, R.D., PICCOLI, H.M., HANSKI, E., NISBET, E.G., WATERTON, P., PEARSON, D.G., ANBAR, A.D. (2019) Secular mantle oxidation across the Archean-Proterozoic boundary: Evidence from V partitioning in komatiites and picrites. *Geochimica et Cosmochimica Acta* 250, 49-75.
- NISBET, E.G., CHEADLE, M.J., ARNDT, N.T., BICKLE, M.J. (1993) Constraining the Potential Temperature of the Archean Mantle - a Review of the Evidence from Komatiites. *Lithos* 30, 291-307.
- OPPENHEIMER, C., SCAILLET, B., WOODS, A., SUTTON, A.J., ELIAS, T., MOUSSALLAM, Y. (2018) Influence of eruptive style on volcanic gas emission chemistry and temperature. *Nature Geoscience* 11, 678-681.
- OSTRANDER, C.M., NIELSEN, S.G., OWENS, J.D., KENDALL, B., GORDON, G.W., ROMANIELLO, S.J., ANBAR, A.D. (2019) Fully oxygenated water columns over continental shelves before the Great Oxidation Event. *Nature Geoscience* 12, 186-191.
- PAVLOV, A.A., KASTING, J.F. (2002) Mass-independent fractionation of sulfur isotopes in Archean sediments: Strong evidence for an anoxic Archean atmosphere. *Astrobiology* 2, 27-41.
- PLANAVSKY, N.J., ASAEL, D., HOFMANN, A., REINHARD, C.T., LALONDE, S.V., KNUDSEN, A., WANG, X.L., OSSA, F.O., PECOITS, E., SMITH, A.J.B., BEUKES, N.J., BEKKER, A., JOHNSON, T.M., KONHAUSER, K.O., LYONS, T.W., ROUXEL, O.J. (2014) Evidence for oxygenic photosynthesis half a billion years before the Great Oxidation Event. *Nature Geoscience* 7, 283-286.
- SATKOSKI, A.M., BEUKES, N.J., LI, W.Q., BEARD, B.L., JOHNSON, C.M. (2015) A redox-stratified ocean 3.2 billion years ago. *Earth and Planetary Science Letters* 430, 43-53.
- SCHIRRMESTER, B.E., GUGGER, M., DONOGHUE, P.C.J. (2015) Cyanobacteria and the Great Oxidation Event: evidence from genes and fossils. *Palaeontology* 58, 769-785.
- SLEEP, N.H. (2005) Dioxygen over geological time. *Biogeochemical Cycles of Elements* 43, 49-73.
- SLEEP, N.H. (2018) Geological and Geochemical Constraints on the Origin and Evolution of Life. *Astrobiology* 18, 1199-1219.
- ZAHNLE, K., CLAIRE, M., CATLING, D. (2006) The loss of mass-independent fractionation in sulfur due to a Palaeoproterozoic collapse of atmospheric methane. *Geobiology* 4, 271-283.

■ Mantle cooling causes more reducing volcanic gases and gradual reduction of the atmosphere

S. Kadoya, D.C. Catling, R.W. Nicklas, I.S. Puchtel, A.D. Anbar

■ Supplementary Information

The Supplementary Information includes:

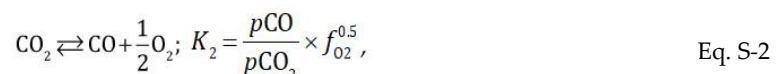
- S-1 Model Description
- S-2 Temperature Dependence of the QFM Buffer and Equilibrium Constants
- S-3 Temperature Dependence of Gas Composition
- S-4 Temperature Dependence of Oxygen Fugacity
- S-5 Temperature Dependence of Oxygenation Parameter
- S-6 Another Effect of Temperature Decrease
- S-7 Sensitivity Test to the Organic Burial Fraction (f_{org})
- S-8 Effect of Pressure
- Figures S-1 to S-9
- Supplementary Information References

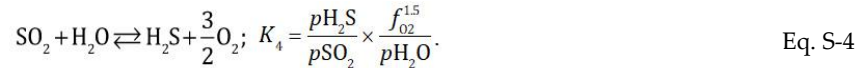
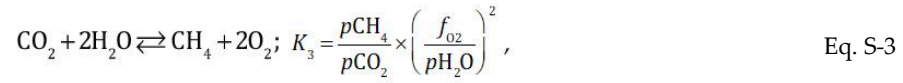
S-1 Model Description

In this study, we calculate the volcanic gas composition, the source and sink of oxygen, and the oxygenation parameter as a function of temperature. Here, we describe each model in this order.

S-1.1 Volcanic gas composition

We assumed that a volcanic gas mixture is composed of H_2O , H_2 , CO_2 , CO , CH_4 , SO_2 , and H_2S , and is in thermodynamic equilibrium. The thermodynamic equilibrium is described as follows:





Here, we assume that all fugacities are equal to their partial pressure and introduce the oxygen fugacity (f_{O_2}). We calculate the equilibrium constants of above equations using data of Chase and National Institute of Standards and Technology (U.S.) (1998).

In addition, we set the total pressure of volcanic gas at 5 bar ($\equiv P_{\text{tot}}$) which corresponds to release from subaerial volcanoes (Holland, 1984, p. 47): *i.e.*

$$p\text{H}_2\text{O} + p\text{H}_2 + p\text{CO}_2 + p\text{CO} + p\text{CH}_4 + p\text{SO}_2 + p\text{H}_2\text{S} = P_{\text{tot}} \quad \text{Eq. S-5}$$

Additionally, we conserve in hydrogen, carbon, and sulfur fluxes:

$$F_{\text{H}_2\text{O}} + F_{\text{H}_2} + 2F_{\text{CH}_4} + F_{\text{H}_2\text{S}} = F_{\text{hydrogen}}, \quad \text{Eq. S-6}$$

$$F_{\text{CO}_2} + F_{\text{CO}} + F_{\text{CH}_4} = F_{\text{carbon}}, \quad \text{Eq. S-7}$$

$$F_{\text{SO}_2} + F_{\text{H}_2\text{S}} = F_{\text{sulfur}}. \quad \text{Eq. S-8}$$

Here, for example, $F_{\text{H}_2\text{O}}$ represents the flux of H_2O . According to the modern global fluxes summarised in Catling and Kasting (2017), modern fluxes, F_{hydrogen} , F_{carbon} , and F_{sulfur} , are 97 Tmol/yr, 9 Tmol/yr, and 2.2 Tmol/yr, respectively. In addition, we assumed that the relationship between partial pressure and flux of each gas species (*e.g.*, H_2O) can be written as:

$$p\text{H}_2\text{O} = \frac{F_{\text{H}_2\text{O}}}{F_{\text{tot}}} \times P_{\text{tot}}, \quad \text{Eq. S-9}$$

Here, F_{tot} is the total gas flux; *i.e.*

$$F_{\text{tot}} \equiv F_{\text{H}_2\text{O}} + F_{\text{H}_2} + F_{\text{CO}_2} + F_{\text{CO}} + F_{\text{CH}_4} + F_{\text{SO}_2} + F_{\text{H}_2\text{S}}. \quad \text{Eq. S-10}$$

In order to solve the above equations, we need one more equation. In this study, we apply two different assumptions. For one case, we assumed that gas is buffered by the surrounding melt: *i.e.* the oxygen fugacity of the gas phase is equal to that of the surrounding melt. This case is the "buffered system" case. In addition, we assumed that the oxygenation state of the melt (*i.e.* the difference in oxygen fugacity from the QFM buffer) is constant. For the consistency with another case, we represent the oxygenation state as ΔQFM_{2000} that is the ΔQFM at 2000 K. Hence, the oxygen fugacity is given as follows:

$$\log_{10} f_{\text{O}_2} = \log_{10} f_{\text{O}_2, \text{qfm}} + \Delta\text{QFM}_{2000}. \quad \text{Eq. S-11}$$

The oxygen fugacity of QFM buffer ($f_{\text{O}_2, \text{qfm}}$) is calculated by the equation given by Wones and Gilbert (1969).

For another case, we assumed that reactions between gases of a volcanic gas mixture occur in a closed system. This case is named as the "closed system" case. No constituent enters or leaves the closed system, so the mass of oxygen in terms of moles O_2 is conserved as follows:

$$\frac{1}{2}F_{\text{H}_2\text{O}} + F_{\text{CO}_2} + \frac{1}{2}F_{\text{CO}} + F_{\text{SO}_2} \equiv F_{\text{oxygen}}. \quad \text{Eq. S-12}$$

Here, the constant of F_{oxygen} is a free parameter. To compare the closed and buffered systems, we set F_{oxygen} so that the oxygen fugacity of the closed system is equal to that of the buffered system at 2000 K. As explained above, the oxidation state (*i.e.* ΔQFM) at 2000 K is denoted as ΔQFM_{2000} .

S-1-2 Sources and sinks of oxygen

It is necessary to define reference oxidation states for volatile species in order to analyze the global redox budget. We take H_2O ,



CO₂ and SO₂ to be redox neutral, which means that their entry or exit from the atmosphere does not change the redox budget. With this convention, H₂, CO, CH₄ and H₂S are sinks of atmospheric oxygen with net photochemical reactions as follows:



Hence, for example, 1 mol of H₂ degassing corresponds to 0.5 mol of O₂ consumption.

On the other hand, the burial of organic matter from oxygenic photosynthesis denoted as carbohydrate (CH₂O) is a source of oxygen:



In addition, the reduction of SO₂ followed by the burial of pyrite is as a source of oxygen as follows:



Also, the net reaction of H₂S can be written combining Eq. S-16 and S-18:



Hence, the net effect of the degassing of 1 mol H₂S is 0.25 mol O₂ sink.

Summarising above, the source (F_{source}) and sink (F_{sink}) of oxygen can be written as follows:

$$F_{\text{source}} = f_{\text{org}} \times (F_{\text{CO}_2} + F_{\text{CO}} + F_{\text{CH}_4}) + \frac{5}{4}F_{\text{SO}_2}, \quad \text{Eq. S-20}$$

$$F_{\text{sink}} = \frac{1}{2}F_{\text{H}_2} + \frac{1}{2}F_{\text{CO}} + 2F_{\text{CH}_4} + \frac{1}{4}F_{\text{H}_2\text{S}}. \quad \text{Eq. S-21}$$

For simplicity, we set the organic burial fraction (f_{org}) at 20 %, which is the canonical value, but test the sensitivity to this parameter in Section S-7.

S-1.3 Oxygenation parameter

According to Catling and Claire (2005), the oxygenation parameter (K_{oxy}) is defined as a ratio of the O₂ flux to the atmosphere, F_{source} , to the flux of kinetically rapid sinks, F_{sink} , where the latter can contain excess reductants above those needed to consume the O₂ flux, *i.e.*

$$K_{\text{oxy}} \equiv \frac{F_{\text{source}}}{F_{\text{sink}}}. \quad \text{Eq. S-22}$$

In this paper, F_{sink} is considered to be dominated by oxidisable volcanic gases because we are explicitly considering the effect of volcanic gases on the oxygenation of the atmosphere. Consequently, we don't consider processes that depend on redox state of the surface. The F_{source} term doesn't include hydrogen escape to space because escape occurs under reducing conditions. The hydrogen escape rate depends on the concentration of H-bearing compounds, such as H₂ and CH₄ (*e.g.*, Catling *et al.*, 2001). Also, F_{sink} doesn't include oxidative weathering of the crust because oxidative weathering only occurs under oxidising conditions and is negligible before the GOE (Sleep, 2004; Claire *et al.*, 2006). Even in the marine realm, the ratio of Fe³⁺ / total Fe is far lower in Archean iron formations than in late Proterozoic ones (Klein *et al.*, 1992), which indicates that less iron was oxidised in the Archean than in the Proterozoic.

When $K_{\text{oxy}} < 1$, the flux of oxidisable volcanic gases exceeds the O₂ flux and the atmosphere is anoxic; excess hydrogen



accumulates until balanced by a continuous hydrogen escape flux. When $K_{\text{oxy}} < 1$, oxidative weathering is negligible because of the lack of atmospheric O_2 . When $K_{\text{oxy}} > 1$, the O_2 source exceeds the flux of oxidisable volcanic gases and O_2 accumulates until balanced by oxidative weathering. In the oxic atmosphere, the hydrogen escape flux is far lower than that in the anoxic atmosphere. How various source and sink fluxes of O_2 evolve and how K_{oxy} changes with time has been demonstrated in the results of the oxygen model of Claire *et al.* (2006). We note that in the post-GOE world, the volcanic edifices themselves become O_2 sinks in addition to oxidisable volcanic gases (Sleep, 2005). The erosion of volcanoes, and the availability of ferrous iron in particular, would be an oxidative weathering sink for O_2 . Indeed, it is possible that a feedback with oxidative weathering forced the levels of mid-Proterozoic O_2 to remain well below modern, although incomplete oxidative weathering of organic carbon has been proposed as the main contributor rather than ferrous iron (Daines *et al.*, 2017).

F_{source} and F_{sink} are defined as Eq. S-20 and S-21, then Eq. S-22 can be written as follows:

$$K_{\text{oxi}} = \frac{4f_{\text{org}} \times (F_{\text{CO}_2} + F_{\text{CO}} + F_{\text{CH}_4}) + 5F_{\text{SO}_2}}{2F_{\text{H}_2} + 2F_{\text{CO}} + 8F_{\text{CH}_4} + F_{\text{H}_2\text{S}}} \quad \text{Eq. S-23}$$

Since all fluxes can be written using their partial pressure, P_{tot} and F_{tot} , e.g., $F_{\text{H}_2\text{O}} = (p_{\text{H}_2\text{O}} / P_{\text{tot}}) \times F_{\text{tot}}$, Eq. S-23 can be re-written as follows:

$$K_{\text{oxy}} = \frac{4f_{\text{org}} \times (p_{\text{CO}_2} + p_{\text{CO}} + p_{\text{CH}_4}) + 5p_{\text{SO}_2}}{2p_{\text{H}_2} + 2p_{\text{CO}} + 8p_{\text{CH}_4} + p_{\text{H}_2\text{S}}} \quad \text{Eq. S-24}$$

S-2 Temperature Dependence of QFM buffer and Equilibrium Constants

If we assume that the mantle is buffered close to the Quartz-Fayalite-Magnetite (QFM) redox buffer, mantle cooling decreases the absolute oxygen fugacity (f_{O_2}), as shown in Figure S-1a; but the cooling also affects the equilibrium constants of the redox speciation reactions of C, S, and H gases (Fig. S-1b). These two effects must be convolved to determine the net effect of mantle cooling on the redox state of the atmosphere.

Under these conditions, a decrease in equilibrium constant favors reaction to the left. For example, cooling favors H_2O more than H_2 in the reaction $\text{H}_2\text{O} \leftrightarrow \text{H}_2 + 0.5 \text{O}_2$, whose equilibrium constant is shown by solid line in Figure S-1b. However, the actual ratio of partial pressures, (e.g., $p_{\text{H}_2} / p_{\text{H}_2\text{O}}$) can depend more on the temperature-dependence of oxygen fugacity, as we illustrate below.

Figure S-1c shows the ratio of the partial pressures of volcanic gases as a function of temperature, assuming that the f_{O_2} value follows the QFM buffer and accounting for temperature-dependent equilibria (*i.e.* Fig. S-1a). As shown in Figure S-1c, cooling decreases the ratio of $p_{\text{CO}} / p_{\text{CO}_2}$ (dotted line). Cooling also decreases the ratio of $p_{\text{H}_2} / p_{\text{H}_2\text{O}}$ (solid line), but the change is more moderate for $p_{\text{H}_2} / p_{\text{H}_2\text{O}}$ than for $p_{\text{CO}} / p_{\text{CO}_2}$ (Fig. S-1c). In contrast, cooling increases the ratios of $p_{\text{H}_2\text{S}} / (p_{\text{SO}_2} p_{\text{H}_2\text{O}})$ (dash-dot line in Fig. S-1c). The decrease in temperature also increases $p_{\text{CH}_4} / (p_{\text{CO}_2} (p_{\text{H}_2\text{O}})^2)$ (dashed line in Fig. S-1c). However, as indicated by Figure S-1b and S-1c, the concentration of methane is essentially negligible. Hence, cooling causes the oxidation of CO to CO_2 and the reduction of SO_2 to H_2S .



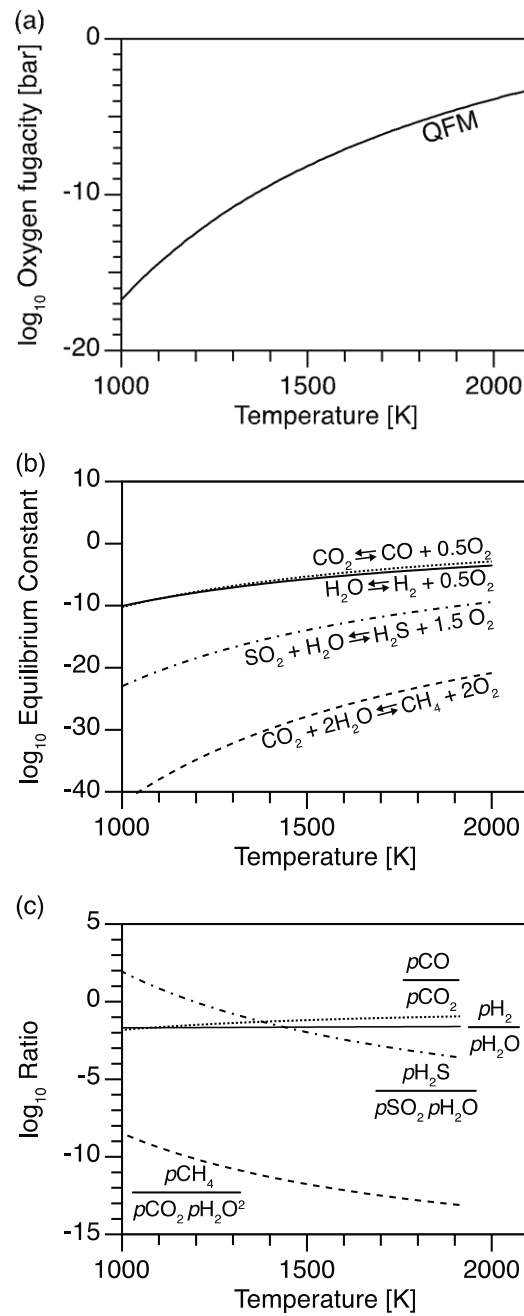


Figure S-1 (a) Oxygen fugacity of the Quartz-Fayalite-Magnetite (QFM) buffer, (b) equilibrium constant, and (c) ratio of the partial pressure of each volcanic gas, as a function of temperature. In (c), we assume that oxygen fugacity follows the QFM buffer (*i.e.* Fig. S-1a).



S-3 Temperature Dependence of Gas Composition

Long-term cooling of the planetary interior changes thermodynamic equilibrium among gases. Hence, the composition of volcanic gases should change with time even if other parameters remain constant. Figure S-2 shows the volcanic gas composition as a function of temperature. Here, the reference oxygen fugacity is set at $\Delta QFM_{2000} = 0$ at 2000 K. In other words, we assumed QFM buffer for the buffered system (Fig. S-2a).

For both cases of the buffered system and the closed system, cooling decreases CO and increases CO₂ (Fig. S-2). This is because cooling favors CO₂ more than CO, which is indicated by the decrease in equilibrium constant of a reaction involving carbon with the decrease in temperature (dashed line in Fig. S-3). Thus, the ratio of p_{CO} to p_{CO_2} decreases (*i.e.* more oxidative) with cooling (Fig. S-2; see also the dotted line in Fig. S-1c).

On the other hand, cooling decreases SO₂ and increases H₂S for both cases of the buffered system and the closed system (Fig. S-2). This is because cooling favors H₂S more than SO₂, which is indicated by the increase in equilibrium constant of a reaction involving sulfur with cooling (solid line in Fig. S-3). Thus, the ratio of p_{H_2S} to p_{SO_2} increases (*i.e.* more reductive) with cooling (Fig. S-2; see also the dash-dot line in Fig. S-1c).

The main difference between the buffered and closed systems lies in the temperature dependence of hydrogen and sulfur. So, we focus on the following reaction:



As explained above, cooling increases the ratio of p_{H_2S} to p_{SO_2} for both systems. However, while cooling changes the dominant species of sulfur from SO₂ to H₂S for the buffered system (Fig. S-2a), SO₂ and H₂S are comparable even at low temperature (~1000 K) for the closed system (Fig. S-2b). On the other hand, cooling decreases H₂ more for the closed system (Fig. S-2b) than for the buffered system (Fig. S-2a).

The difference in hydrogen and sulfur (Fig. S-2) results from the difference in the assumption between the buffered and closed systems. For the buffered system, the oxygen fugacity of the gas is equal to the oxygen fugacity of the melt by definition. Hence, the ratio of p_{H_2} to p_{H_2O} in the buffered system is set by the following equation (see also Eq. S-1):

$$\log_{10} \frac{p_{H_2O}}{p_{H_2}} = K_1 + \frac{1}{2} \log_{10} f_{O_2, \text{melt}} \quad \text{Eq. S-26}$$

In other words, the H₂ decrease due to reduction of SO₂ to H₂S (Eq. S-25) is buffered by reduction of H₂O to H₂ (*i.e.* H₂O → H₂ + 0.5 O₂) while oxygen is consumed by the melt. Therefore, the change in the ratio of p_{H_2O}/p_{H_2} due to the temperature change is moderate for the buffered system (dashed line in Fig. S-4). In addition, cooling can result in the reduction of all SO₂ to H₂S (Fig. S-2a) because of the large change in the equilibrium constant (solid line in Fig. S-3).

On the other hand, for the closed system, the reduction of SO₂ to H₂S is accompanied by the oxidation of H₂O as for the buffered system, but the oxygen fugacity is not buffered. Hence, cooling results in the decrease of H₂ and SO₂, and an increase in H₂S (Fig. S-2b) following reaction Eq. S-25 and temperature dependence of the equilibrium constant (solid line in Fig. S-3). Since the amount of H₂ is limited and not buffered by the melt, the reduction of SO₂ to H₂S due to cooling is incomplete (Fig. S-2b). In addition, cooling increases the ratio of p_{H_2O} to p_{H_2} much more for the closed system than for the buffered system (Fig. S-4).

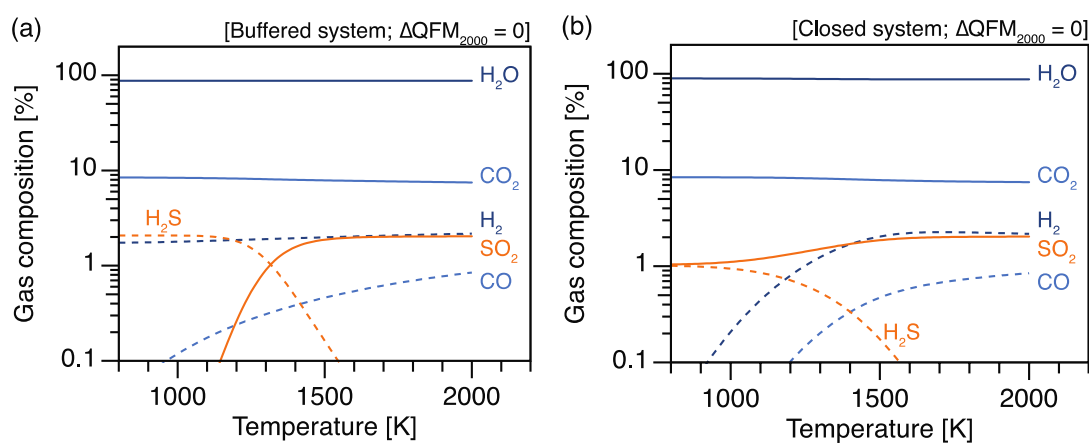


Figure S-2 Gas composition of (a) the buffered system and (b) the closed system of volcanic gases, as a function of temperature. Here, the reference oxygen fugacity (ΔQFM_{2000}) is set at 0. Solid lines represent neutral or oxidative gas, and dashed lines represent reductive gas. Cooling decreases H₂ and CO. On the other hand, the decrease in temperature decreases SO₂ and increases H₂S. In particular for the buffered system case (a), all of the sulfur is SO₂ under high temperature (~2000 K) and H₂S under low temperature (~1000 K). These changes due to temperature are caused by the temperature dependence of equilibrium constant (Fig. S-3).



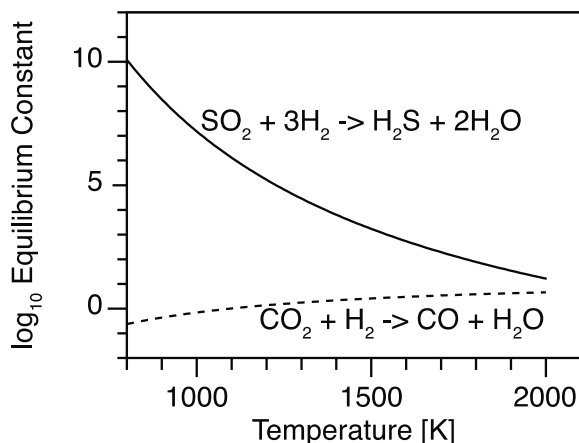


Figure S-3 Equilibrium constant as a function of temperature. Cooling increases the ratio of p_{H_2S} / p_{SO_2} (solid line). On the other hand, cooling decreases the ratio of p_{CO} / p_{CO_2} (dashed line).

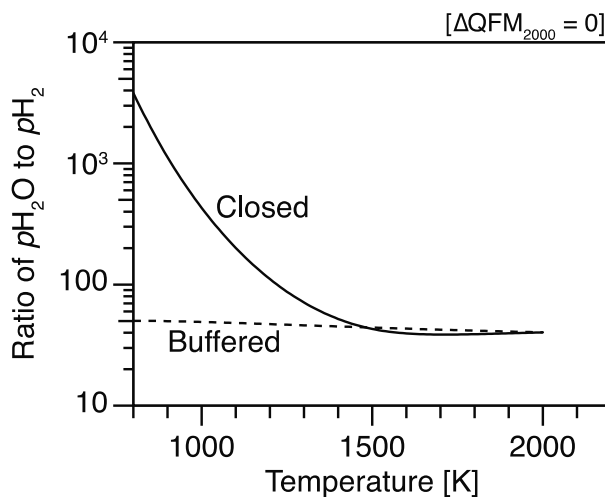


Figure S-4 Ratio of p_{H_2O} to p_{H_2} as a function of temperature. Here, the reference ΔQFM (ΔQFM_{2000}) is set at 0. The decrease in temperature makes the ratio of the closed system larger than the ratio of the buffered system, which corresponds to the increase in ΔQFM of the closed system (see also Eq. S-29).

S-4 Temperature Dependence of Oxygen Fugacity

S-4.1 Temperature dependence of the closed system of volcanic gas

As shown in Figure 1a and Moussallam *et al.* (2019), ΔQFM of the closed system tends to increase with cooling. This is due to the temperature dependence of the gas composition, especially the ratio of p_{H_2O} / p_{H_2} as equilibrium constants change with temperature.

The oxygen fugacity of the closed system of gas can be calculated as follows:

$$\log_{10} f_{O_2, \text{closed}} = 2 \left\{ \log_{10} K_{\text{eq}} + \log_{10} \left(\frac{p_{H_2O}}{p_{H_2}} \right)_{\text{closed}} \right\}. \tag{Eq. S-27}$$

Similarly, the oxygen fugacity of the buffered system can be calculated as follows:

$$\log_{10} f_{O_2, \text{buffered}} = \log_{10} f_{O_2, \text{QFM}} + \Delta QFM_{\text{buffered}} = 2 \left\{ \log_{10} K_{\text{eq}} + \log_{10} \left(\frac{p_{H_2O}}{p_{H_2}} \right)_{\text{buffered}} \right\}. \tag{Eq. S-28}$$



Therefore, ΔQFM of the closed system is calculated using Eq. S-27 and S-28 as follows:

$$\Delta QFM_{\text{closed}} = \Delta QFM_{\text{melt-buffer}} + 2 \left\{ \log_{10} \left(\frac{p\text{H}_2\text{O}}{p\text{H}_2} \right)_{\text{closed}} - \log_{10} \left(\frac{p\text{H}_2\text{O}}{p\text{H}_2} \right)_{\text{melt-buffer}} \right\}. \quad \text{Eq. S-29}$$

As shown in Fig. S-4, cooling increases the ratio of $p\text{H}_2\text{O} / p\text{H}_2$ much more for the closed-system than for the buffered system. Hence, cooling results in higher ΔQFM for the closed system than for the buffered system.

S-4.2 Temperature dependence of oxygen fugacity for the case excluding sulfur

As explained, the increase in ΔQFM with cooling for the closed system results from the increase in the ratio of $p\text{H}_2\text{O}$ to $p\text{H}_2$. Also, the increase in the ratio of $p\text{H}_2\text{O}$ to $p\text{H}_2$ results from the consumption of H_2 via the reaction of Eq. S-25. Therefore, the change in ΔQFM is mainly caused by the reaction involving sulfur (Eq. S-25).

To highlight this point, Figure S-5 compares ΔQFM of two cases for the closed-system case. For one case, we include the sulfur-containing species (*i.e.* SO_2 and H_2S) in addition to other gas species (*i.e.* H_2O , H_2 , CO_2 , CO , and CH_4). For another case, we exclude the sulfur-containing species and consider only other gas species. For the sulfur-including case (solid line in Fig. S-5), cooling increases ΔQFM as explained above.

On the other hand, for the sulfur-excluding case (dashed line in Fig. S-5), cooling slightly decreases ΔQFM . Such a decrease in ΔQFM (*i.e.* decrease in the ratio of $p\text{H}_2\text{O}$ to $p\text{H}_2$) results from the reduction of H_2O to H_2 via the reaction of $\text{CO}_2 + \text{H}_2 = \text{CO} + \text{H}_2\text{O}$. Note that low temperature favors CO_2 and H_2 , as indicated by the dashed line in Figure S-3.

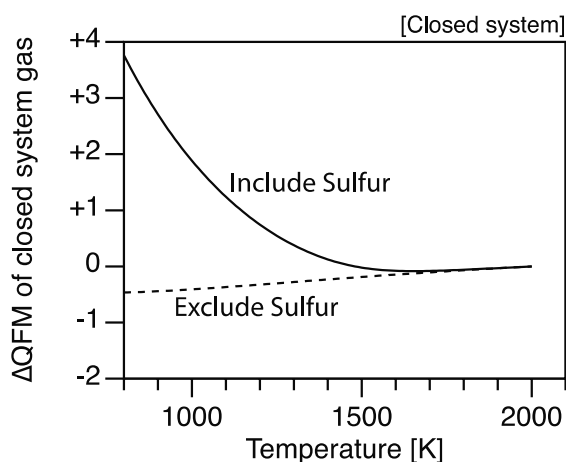


Figure S-5 Oxygen fugacity represented as the difference from QFM buffer level in \log_{10} units (*i.e.* ΔQFM). The closed system is assumed. Considering sulfur-containing species (*i.e.* SO_2 and H_2S), cooling decreases and then increases ΔQFM (solid line; see also Fig. 3a). On the other hand, if we exclude sulfur-containing species, ΔQFM monotonically decreases with cooling (dashed line).

S-5 Temperature Dependence of Oxygenation Parameter

Since the thermal evolution of planetary interior (*i.e.* cooling) changes the volcanic gas composition as explained above, the evolution also changes the capability of volcanic gases to act as a sink of O_2 , *i.e.* affects the oxygenation parameter, K_{oxy} , as shown in Figures 1b and 2b.

As explained above, cooling decreases $p\text{CO}_2 / p\text{CO}$ and increases $p\text{H}_2\text{S} / p\text{SO}_2$ (Fig. S-2) following the temperature dependence of equilibrium constants (Fig. S-3). Hence, cooling decreases the oxygen source flux (F_{source}) owing to the decrease in the flux of SO_2 (Fig. S-6; see also Fig. S-2). However, the organic burial flux is assumed constant since the total carbon flux and the fraction buried as organic carbon are assumed constant. Therefore, F_{source} reaches a constant value asymptotically at low temperature (Fig. S-6a and S-6b).

On the other hand, cooling decreases the oxygen sink flux (F_{sink}) owing to the decrease in the flux of CO , especially under high temperature (~ 1800 K) as shown in Figure S-6a and S-6b (see also Fig. S-2). However, further decrease in temperature (~ 1000 K) increases the flux of H_2S , hence the F_{sink} also reaches asymptotically a constant value (Fig. S-6a and S-6b; see also Fig. S-2). Such non-linear change in F_{source} and F_{sink} also causes the non-linear change in K_{oxy} ($= F_{\text{source}} / F_{\text{sink}}$) as shown in Figure 1b and 2b.



As shown, the non-linear change of K_{oxy} results from the temperature dependence of the reaction involving sulfur (Eq. S-25). Hence, if we exclude sulfur-containing species (*i.e.* SO_2 and H_2S), the decrease in temperature even increases K_{oxy} monotonically (dashed line in Fig. S-7). This is because the temperature decrease favors H_2O and CO_2 more than H_2 and CO , respectively (See Fig. S-1c).

Thus, the evolution of K_{oxy} strongly depends on the redox speciation of sulfur gases.

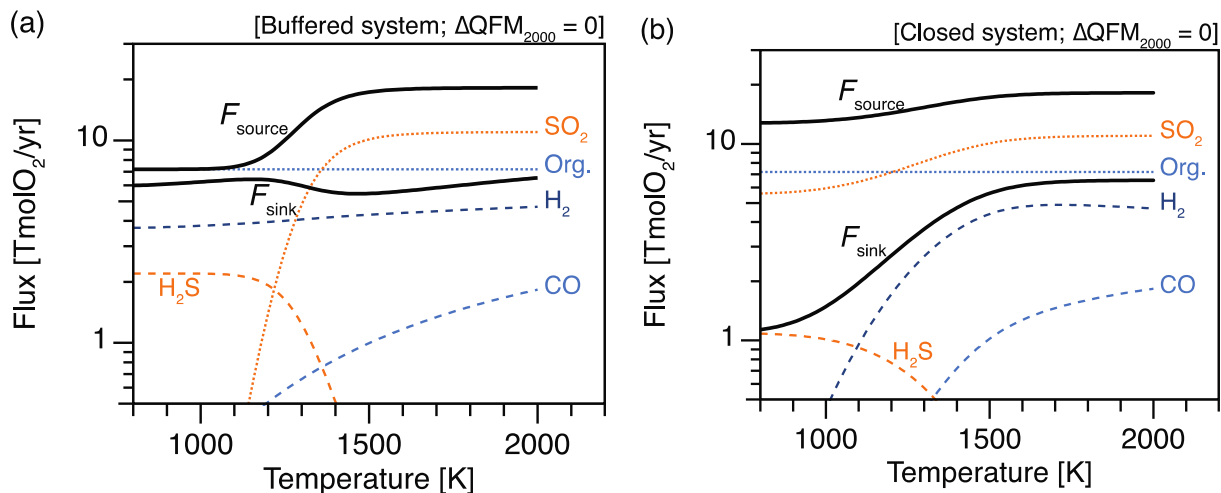


Figure S-6 Fluxes in the units of TmolO₂/yr as a function of temperature: (a) for the buffered system and (b) for the closed system. Here, the reference ΔQFM (ΔQFM₂₀₀₀) is set at 0. Dotted lines represent the oxidative gas flux, and dashed lines represent the reductive gas flux. The ratio of the oxygen source (F_{source}) to kinetically rapid oxygen sink (F_{sink}) from reducing gases is the oxygenation parameter (K_{oxy}). Cooling decreases the flux of H_2 and CO (See also Fig. S-2). Hence, cooling decreases F_{sink} , especially at high temperature (~2000 K) (a and b). On the other hand, cooling increases the flux of H_2S as shown in (a) and (b). Hence, F_{sink} asymptotically reaches a constant value for the closed system under low temperature (b). For the buffered system, F_{sink} even increases under low temperature (a). Cooling also decreases the flux of SO_2 . Hence, F_{source} decreases with cooling (a and b). However, since the flux of organic burial is assumed constant here, F_{source} asymptotically reaches a constant value with cooling (a and b). Such non-linear change in F_{source} and F_{sink} causes the step-like change in K_{oxy} as shown in Figures 1b, 2b, and S-7. Note that K_{oxy} is the ratio of F_{source} to F_{sink} .

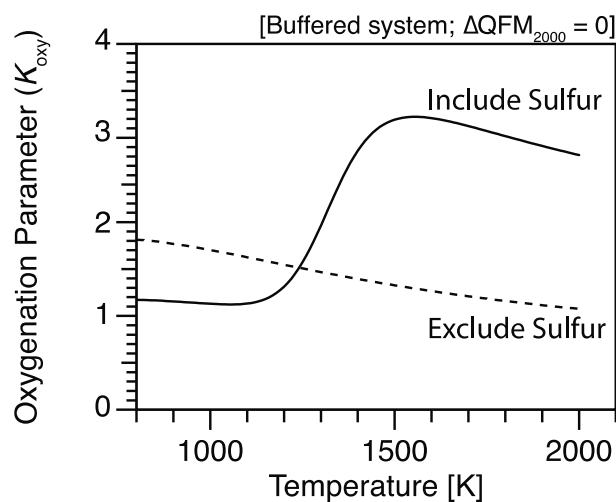


Figure S-7 Oxygenation parameter (K_{oxy}) as a function of temperature. Here, the buffered (system and QFM buffer is assumed. Including sulfur-containing species (*i.e.* SO_2 and H_2S), K_{oxy} decreases with the decrease in temperature (solid line) as shown in Figure 2b. On the other hand, excluding sulfur-containing species, K_{oxy} monotonically increases with the decrease in temperature (dashed line).

S-6 Another Effect of Temperature Decrease

One caveat of this study lies in the potential decrease in serpentinisation with secular cooling. As discussed in Kasting (2013), mantle cooling should have decreased the depth of partial melting. Hence, in the past, *i.e.* when mantle temperature was higher



than the present, the oceanic crust should have been thicker and more mafic than present. This trend for the oceanic crust would decrease the H_2 release via serpentinisation, *i.e.* the sink of O_2 , with time. The modern H_2 flux *via* serpentinisation corresponds to $0.2 \text{ TmolO}_2/\text{yr}$. On the other hand, the sink of O_2 is in the order of $\sim 1 \text{ TmolO}_2/\text{yr}$ (*e.g.*, Fig. S-6). Hence, if the H_2 flux via serpentinisation was larger by an order of magnitude or more and then decreased with time, the decrease in serpentinisation caused by temperature decrease might oxidise the Earth's surface (Kasting, 2013). However, the extent of the change in serpentinisation remains uncertain.

S-7 Sensitivity Test to the Organic Burial Fraction (f_{org})

The oxygenation parameter (K_{oxy}) depends on the organic burial fraction (f_{org}) as shown in Eq. S-24. Figure S-8 shows the effect of f_{org} on K_{oxy} . Here, we vary f_{org} from 10 % to 30 %, which roughly corresponds to the evolutionary range of f_{org} from 3.6 Ga to the present (Krissansen-Totton *et al.*, 2015).

The larger f_{org} results in larger K_{oxy} as shown in Figure S-8 and also in the previous work (Krissansen-Totton *et al.*, 2015). However, the difference in f_{org} does not change the overall effect of cooling on the K_{oxy} . Namely, for the buffered system, cooling decreases K_{oxy} (Fig. S-8a). On the other hand, for the closed system, an initial K_{oxy} that exceeds unity remains > 1 , and an initial K_{oxy} that is less than unity remains < 1 .

According to Krissansen-Totton *et al.* (2015), the secular increase of f_{org} indicated by geological evidence was not able to cause the Great Oxidation Event (GOE) if the other fluxes were constant and if a conventional carbon cycle model is assumed. Moreover, as explained, the secular cooling of the mantle causes the reduction of a volcanic gas mixture, and therefore, the reduction of atmosphere with time. Hence, we conclude some other mechanisms are required to explain the GOE.

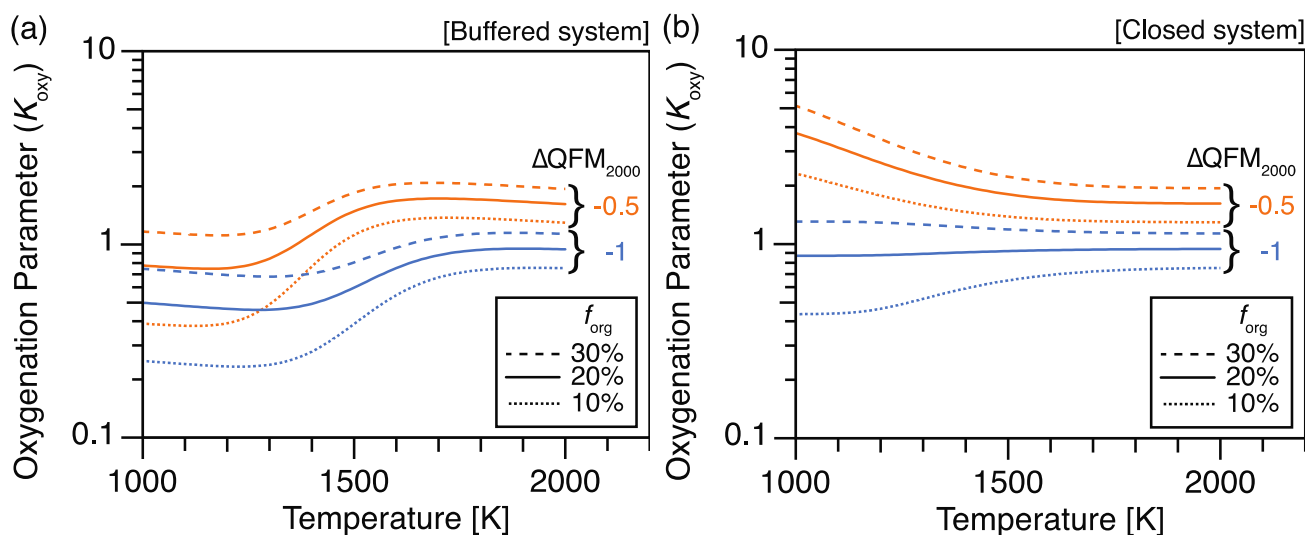


Figure S-8 Oxygenation parameter (K_{oxy}) as a function of temperature: (a) for the buffered system and (b) for the closed system. Orange lines represent the K_{oxy} of $\Delta QFM_{2000} = -0.5$, and blue lines represent the K_{oxy} of $\Delta QFM_{2000} = -1$. Solid lines represent the K_{oxy} of the organic burial fraction ($f_{\text{org}} = 20\%$). On the other hand, dashed lines represent the K_{oxy} of $f_{\text{org}} = 30\%$, and dotted lines represent the K_{oxy} of $f_{\text{org}} = 10\%$. Larger f_{org} results in larger K_{oxy} (a and b). However, difference in f_{org} does not change the conclusion. Namely, for the buffered system, cooling decreases K_{oxy} (a) as shown in Figure 1b. On the other hand, for the closed system, an initial K_{oxy} that exceeds unity remains > 1 , and an initial K_{oxy} that is less than unity remains < 1 (b) as shown in Figure 2b.

S-8 Effect of Pressure

As a nominal case, we set total pressure of volcanic gas, P_{tot} , at 5 bar, assuming an eruption of a subaerial volcano (Holland, 1984, p. 47). However, some have suggested that a higher degassing pressure, such as under submarine conditions, causes more reducing volcanic gas (Kump and Barley, 2007; Gaillard *et al.*, 2011). Here, we investigate the effect of the total pressure of volcanic gas and show that we obtain a similar trend as in previous works.

Figure S-9 shows the mole ratios of reducing gases to their neutral or oxidative equivalent, *e.g.*, H_2 / H_2O . A total pressure of 100 bar results in larger ratios of H_2S / SO_2 and CH_4 / CO_2 than at 5 bar while the ratios of H_2 / H_2O and CO / CO_2 are independent of the total pressure. How the redox state of volcanic gases depends on pressure is mainly affected by the equilibrium state of sulfur because the H_2S / SO_2 ratio is about a few, while CH_4 / CO_2 is much less than unity (Fig. S-9a). Hence, higher total pressure causes more reducing volcanic gas mainly because of the equilibrium state of sulfur, as suggested previously (Kump and Barley, 2007; Gaillard *et al.*, 2011).



The more reducing volcanic gases caused by higher total pressure also produce a lower oxygenation parameter, K_{oxy} (Fig. S-9b). Nonetheless, the temperature dependence of K_{oxy} , *i.e.* the decrease in K_{oxy} with cooling, is similar for both pressure cases. Also, the difference caused by total pressure diminishes at temperatures less than ~ 1200 K (Fig. S-9b). At such low temperature, almost all of sulfur is H_2S for both cases of pressure. Note that at 1000 K, $\text{H}_2\text{S} / \text{SO}_2$ is $\sim 10^3$ for the case of 5 bar and $\sim 10^4$ for the case of 100 bar (Fig. S-9a). Similarly, the difference caused by total pressure diminishes at temperatures exceeding ~ 1900 K (Fig. S-9b) because almost all the sulfur becomes SO_2 (Fig. S-9b).

In summary, we obtained a pressure dependence of the redox state of the volcanic gas that is consistent with previous works (Kump and Barley, 2007; Gaillard *et al.*, 2011). Nonetheless, the temperature dependence of K_{oxy} of the volcanic gas at 5 and 100 bar has similar behavior (Fig. S-9b). Hence, even considering a different pressure regime, the main conclusion of this study does not change.

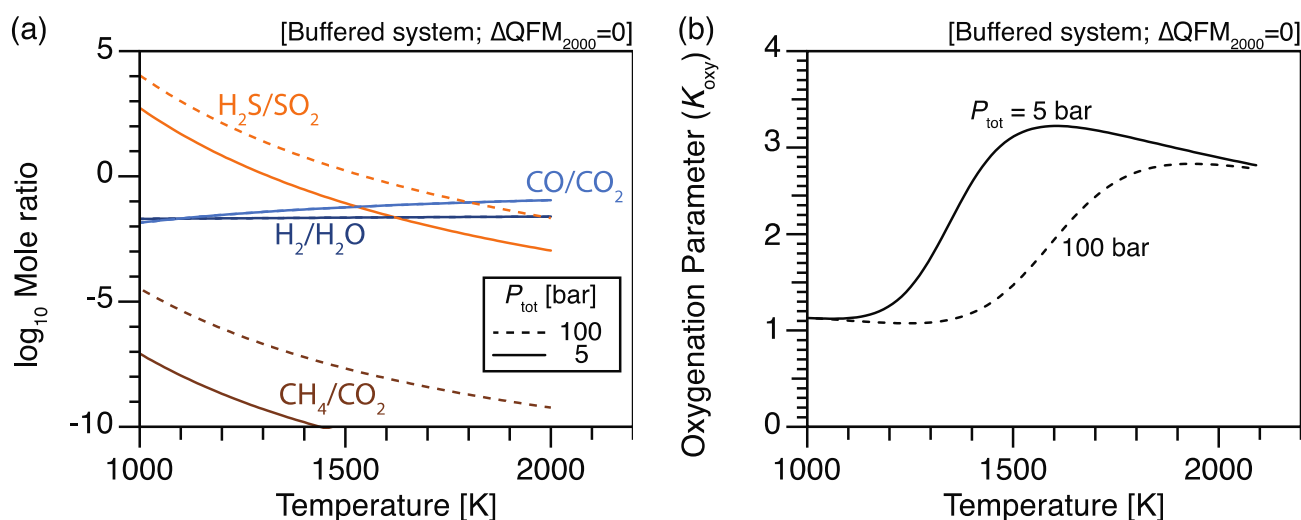


Figure S-9 Effect of total pressure, P_{tot} : (a) volcanic gas mole ratios and (b) the oxygenation parameter (K_{oxy}) as a function of temperature. Here, the buffered system and QFM buffer is assumed. Solid lines represent the case of $P_{\text{tot}} = 5$ bar, and dashed lines represent the case of $P_{\text{tot}} = 100$ bar. Higher P_{tot} results in larger ratios of $\text{H}_2\text{S} / \text{SO}_2$ and $\text{CH}_4 / \text{CO}_2$, *i.e.*, more reducing volcanic gas (a). Hence, higher P_{tot} results in lower K_{oxy} (b).

Supplementary Information References

- Catling, D.C., Claire, M.W. (2005) How Earth's atmosphere evolved to an oxidic state: A status report. *Earth and Planetary Science Letters* 237, 1-20.
- Catling, D.C., Kasting, J.F. (2017) *Atmospheric evolution on inhabited and lifeless worlds*. Cambridge University Press.
- Catling, D.C., Zahnle, K.J., McKay, C.P. (2001) Biogenic methane, hydrogen escape, and the irreversible oxidation of early Earth. *Science* 293, 839-843.
- Chase, M.W., National Institute of Standards and Technology (U.S.) (1998) *NIST-JANAF thermochemical tables*. American Chemical Society; American Institute of Physics for the National Institute of Standards and Technology, Washington, DC, New York.
- Claire, M.W., Catling, D.C., Zahnle, K.J. (2006) Biogeochemical modelling of the rise in atmospheric oxygen. *Geobiology* 4, 239-269.
- Daines, S.J., Mills, B.J.W., Lenton, T.M. (2017) Atmospheric oxygen regulation at low Proterozoic levels by incomplete oxidative weathering of sedimentary organic carbon. *Nature Communications* 8.
- Gaillard, F., Scaillet, B., Arndt, N.T. (2011) Atmospheric oxygenation caused by a change in volcanic degassing pressure. *Nature* 478, 229-U112.
- Holland, H.D. (1984) *The chemical evolution of the atmosphere and oceans*. Princeton University Press, Princeton, N.J.
- Kasting, J.F. (2013) What caused the rise of atmospheric O₂? *Chemical Geology* 362, 13-25.
- Klein, C., Beukes, N.J., Holland, H.D., Kasting, J.F., Kump, L.R., Lowe, D.R. (1992) Proterozoic Atmosphere and Ocean. In: Schopf, J.W. and Klein, C. Eds.), *The Proterozoic Biosphere*. Cambridge University Press, Cambridge, 135-174.
- Krissansen-Totton, J., Buick, R., Catling, D.C. (2015) A Statistical Analysis of the Carbon Isotope Record from the Archean to Phanerozoic and Implications for the Rise of Oxygen. *American Journal of Science* 315, 275-316.
- Kump, L.R., Barley, M.E. (2007) Increased subaerial volcanism and the rise of atmospheric oxygen 2.5 billion years ago. *Nature* 448, 1033-1036.
- Moussallam, Y., Oppenheimer, G., Scaillet, B. (2019) On the relationship between oxidation state and temperature of volcanic gas emissions. *Earth and Planetary Science Letters* 520, 260-267.
- Sleep, N.H. (2004) Archean palaeosols and Archean air. *Nature* 432, 1-1.
- Sleep, N.H. (2005) Dioxygen over geological time. *Biogeochemical Cycles of Elements* 43, 49-73.
- Wones, D.R., Gilbert, M.C. (1969) Fayalite-Magnetite-Quartz Assemblage between 600 Degrees and 800 Degrees C. *American Journal of Science* 267, 480-&

